

# Towards Bose-Einstein Condensation of Excitons

Xin Lu

**Abstract:** A new method to produce long life-time excitons has been employed using the band-gap engineering quantum hetero-structures of 2D coupled quantum wells. Just as atom condensation were performed on atomic gases, confined in the potential traps, the quasi 2D excitons are collected in an in-plane potential trap and PL measurements show that they are indeed condensed at the bottom of the traps, giving rise to a statistically degenerate Bose gas. Meanwhile, the PL kinetics, which is determined by the bosonic stimulated scattering of indirect excitons in CQWs, also indicates condensation to the low energy states. A macroscopically ordered exciton state has been observed. The spatially resolved measurements reveal fragmentation of the ring-shaped emission pattern into circular structures that form periodic arrays over length up to 1mm.

## I. Introduction [15]

Bose-Einstein Condensation (BEC) has called much attention from both experimental and theoretical physicist for many years as a fascinating research area, which may exhibit macroscopic coherence in the form of vortices and superfluidity. Actually, there is a variety of quantum liquids—such as superconductor, liquid helium and atom BEC [1, 2, 3, 4]—which have undergone dramatic progress in experiment. However, experimental observation of macroscopically ordered state in the semiconductors has remained a challenge and relatively unexplored problem for decades. A promising candidate in such a system is excitons, which are the bound pairs of electron and hole that are formed during Laser excitation. At low density, excitons are boson particles [5], and they can condensate to the low-energy state and even lead to BEC [5, 6] just as atoms when lowering the temperature. In fact, the exciton mass is much smaller than atoms and thus BEC should occur at much higher temperature of about 1K than atoms at about several MKs or at much less density. However, unfortunately, the greatest obstacle for excitons to reach BEC condition is their short lifetime: The temperature of excitons in practice can considerably exceed that of the semiconductor lattice, so the lifetime of excitons against electron-hole recombination should be long enough compared with the characteristic timescale for the lattice to cool down the hot photo-generated excitons.

Until now, lots of experimental efforts focus on the exciton BEC in bulk semiconductors dealt mainly with bulk  $Cu_2O$  [7, 8], a material whose ground exciton state is optically dipole-inactive and has, therefore, a very low radiative recombination rate. The expected conditions for the BEC realization appear to be that  $T_c \propto n^{2/3}$  would reach 2.3 K at exciton density  $n = 10^{17} \text{ cm}^{-3}$ . However, meanwhile, a competitive process comes to our view at high density which may undermine the condensation: the exciton Auger recombination rate [9], proportional to  $n$ , which increases faster than  $T_c$  with increasing  $n$ . Recent works in Auger Process indicates that the recombination rate in  $Cu_2O$  is about two orders of magnitude higher than that was assumed before. Thus the exciton densities reached in up-to-date experiments are much far from that required to get degenerated Bose gas of excitons.

A new approach to overcome this barrier has been applied these years with the development of nanostructure techniques: a quasi-two-dimensional gas of indirect excitons in coupled quantum wells (QWs). Because it enables a much longer lifetime and faster cooling rate of excitons, the system is getting more and more favored to accumulate boson particles in the lowest energy states. In fact, great progress has been made to realize the BEC of excitons and many interesting phenomena have been discovered in the last few years.

## II Experiment & Explanation

### 2.1 Method

In contrast to bulk semiconductors, artificially grown semiconductor nanostructure allows us to tune, to some extent, both the mass and the radiative lifetime of excitons. A new arrangement of experiment is employed: an extremely cold (the minimal cryostat temperature  $T=0.05\text{K}$ ) optically pumped high-quality GaAs/AlGaAs coupled quantum well (CQW) in the presence of a static voltage and magnetic field [10].

An  $n^+i-n^+$  GaAs/AlGaAs CQW structure was grown by molecular-beam epitaxy. The  $i$  region consists of a single pair of 8 nm GaAs QWs separated by a 4 nm  $\text{Al}_{0.33}\text{Ga}_{0.67}\text{As}$  barrier and surrounded by 200 nm  $\text{Al}_{0.33}\text{Ga}_{0.67}\text{As}$  barrier layers. The  $n^+$  layers are Si-doped GaAs with  $N_{\text{Si}}=5 \times 10^{17} \text{ cm}^{-3}$ . The electric field in the  $z$  direction is monitored by the external gate voltage  $V_g$  applied between  $n^+$  layers ( $V_g=1\text{V}$ ). The small in-plane disorder in the CQW is indicated by the photoluminescence (PL) linewidth about 1 meV. The 50 ns laser excitation has a rectangular shape with the edge sharpness about 0.5 ns ( $\hbar\omega = 1.85 \text{ eV}$  and the repetition frequency is 1 MHz). The experiment is performed in a  $He^3/He^4$  refrigerator or  $He^4$  cryostat. Excitation and PL collection were performed normal to the CQW plane by means of a 100  $\mu\text{m}$  optical fiber positioned 300  $\mu\text{m}$  above 350\*350  $\mu\text{m}$  mesa (the total sample area was about 4  $\text{mm}^2$ ).

There are two primary advantages of using CQWs for realizing a quantum degenerate exciton gas and, ultimately, the BEC-like phase transition: (1) the long lifetime of indirect excitons and (2) the short exciton cooling time. The long lifetime originates from the spatial separation between the electron and hole layers, resulting in a radiative lifetime which is more than three orders of magnitude longer than that

of direct excitons in single QWs. As for the cooling time, it's due to the relaxation of the momentum conservation law in the  $z$  direction ( $z \perp QW$  plane). As we know, the hot photo-excited excitons are cooled down to the temperature of the cold lattice via emission of bulk longitudinal acoustic phonons. For quasi-two-dimensional systems the ground state mode  $E=0$  couples to the continuum of the energy states  $E>E_0$  rather than to the single energy state  $E=E_0=2Mv_s^2$  ( $v_s$  is the sound velocity) as it occurs in bulk semiconductors. As a result, the characteristic thermalization time of excitons in GaAs QWs is 2-3 orders of magnitude shorter than that in bulk GaAs.

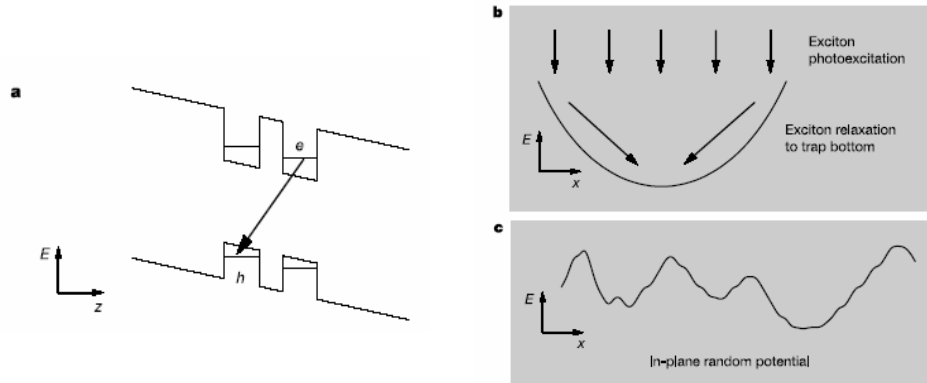


**Fig. 1:** Potential profiles in Coupled quantum well structures in the growth direction  $z$ , and in the  $x$ - $y$  plane. **a**, Energy band diagram of the coupled quantum well (QW) structures. The indirect excitons in coupled QWs are characterized by high cooling rates, three orders of magnitude higher than in bulk GaAs, and long life time, more than three orders of magnitude longer than in a single GaAs QW. The life time is much longer than the characteristic timescale for cooling, so that the exciton temperature can very low, well below 1K. **b**, in-plane

potential of a trap for excitons in QW structure. The conditions for the excitons BEC are significantly improved in such potential traps because of the confinement effect and the enhanced local density driven by the exciton energy relaxation **c**, Schematic of the in-plane potential landscape formed by random potential fluctuations. Such natural local potential minima can host highly degenerate exciton systems and ultimately, BEC.

## 2.2 Condensation in Potential Traps[11]

Just as the advances in BEC of atoms were made possible by exploiting the confinement of atomic gases within potential traps, the conditions for BEC of indirect excitons are significantly improved if the excitons are collected in a local minimum caused by an in-plane modulation of the potential(Fig. 1). Then  $T_c$  increases because of enhancement of the local density at the trap centre that result from the drift of photo-excited excitons towards the bottom of the trap. Actually, the traps can be formed by lateral modulation of the electric field along  $z$ ,  $E_z$ , by application of a local stress or of a local magnetic field. A clear signature of condensation of a degenerate exciton gas in such traps is its strongly in-plane localized photoluminescence (PL) emission peaked at the bottom of the trap.

Using a spatial resolution of 10 $\mu$ m at  $T=1.6$ K, researchers have observed a huge local enhancement of the indirect exciton PL intensity in several 500\*500  $\mu$ m<sup>2</sup> mesas. As shown in Fig. 2(a), under uniform excitation of a whole mesa using a defocused laser, the indirect exciton PL intensity at the centre of a trap is about 30 times higher than that emitted from any other location on the mesa outside the trap.

This clearly demonstrates that the indirect excitons collect at the bottom of the trap, where the exciton density in the traps is estimated  $n_{\text{trap}} \sim 10^{11} \text{ cm}^{-2}$ .

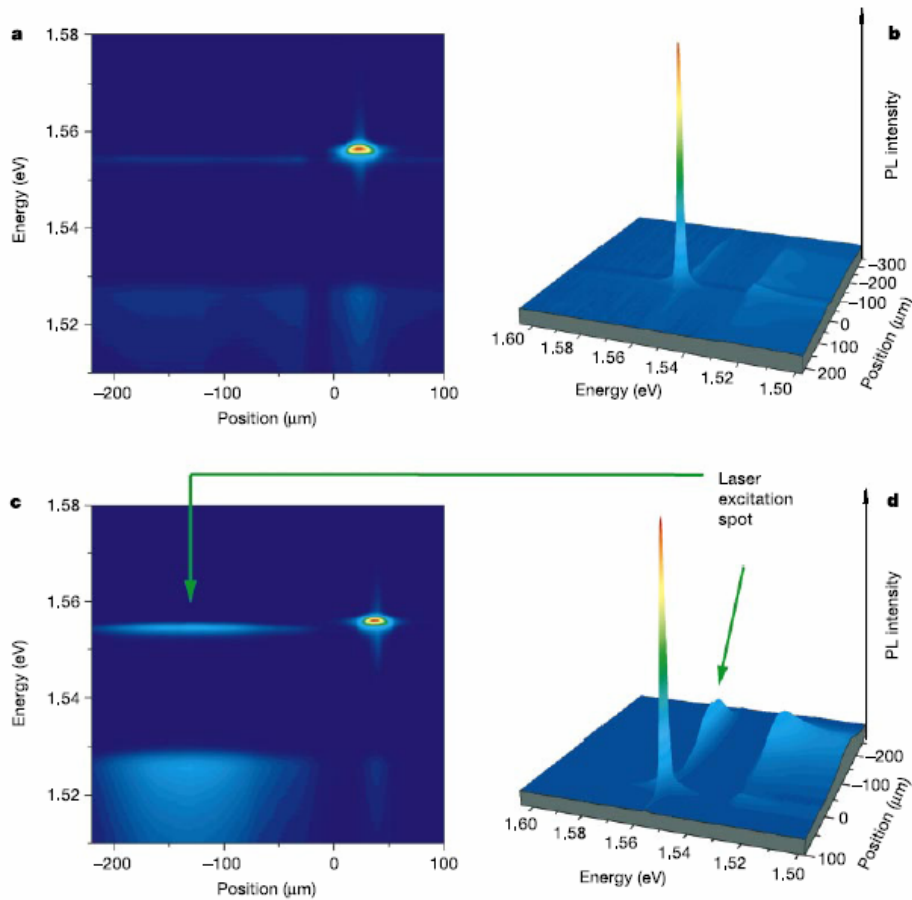


**Fig. 2:** photoluminescence intensity versus energy and one of the in-plane coordinates  $x$  at  $T=1.6\text{K}$  (the PL variation along the orthogonal in  $-y$  plane coordinate  $y$  is the same). The indirect exciton PL line is at about  $1.555\text{eV}$ : the broad line below  $1.53\text{eV}$  comes from bulk  $n^+$ -GaAs emission. **a, b,** The laser excitation spot is defocused and excites the whole  $500 \times 500 \mu\text{m}^2$  mesa. The indirect excitons are

collected in a natural trap resulting in a PL intensity at its centre about 30 times higher than outside. **c, d,** The laser excitation is focused to a spot around  $100 \times 200 \mu\text{m}^2$  about  $170 \mu\text{m}$  away from trap. Even in these conditions the indirect exciton PL intensity at the trap centre is about six times larger than at the centre of the excitation spot. This demonstrates drift and condensation of indirect excitons over macroscopic distances.

The traps under inhomogeneous excitation were explored using a smaller laser spot,  $100 \times 200 \mu\text{m}^2$ , that can be located anywhere on the mesa as far away from the centre as  $400 \mu\text{m}$ . As seen in Fig. 2(b), even in that case the indirect excitons are collected by the trap and the PL intensity from the trap is up to about six times higher than that at the excitation spot. The long lifetime and large diffusion coefficient allows the indirect excitons to travel several hundred micrometers and to be collected in the trap. Especially, during their travel to the trap centre, the initially hot excitons are effectively thermalized down to the lattice temperature via phonon emission. Therefore, in the case of remote excitation, the trap is filled by the cold excitons with the density  $n_{\text{trap}} \sim 1.2 \times 10^{11} \text{ cm}^{-2}$ , which we can get from the exciton density in the laser

spot  $n_{\text{spot}} \sim 2 \cdot 10^{10} \text{ cm}^{-2}$ .

The diameter of the exciton cloud near the bottom of the potential trap deduces as the temperature is lowered, while the peak intensity increases, as shown in Fig. 3. This demonstrates that while at high temperatures the excitons are distributed over the high energy states of the trap, at low T the excitons condense at the bottom of the trap. Similar spatial shrinkage of atom clouds is characteristic of atomic BEC in the potential traps.

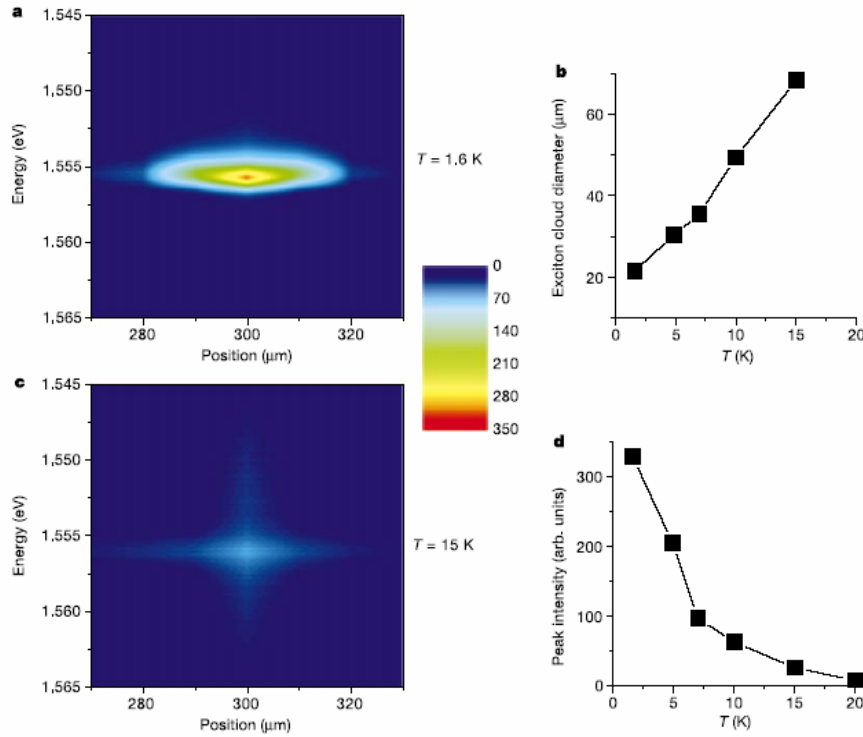


**Fig. 3:** The spatial shrinkage of the exciton cloud near the bottom of the potential trap as the temperature is reduced. **a, c,** Contour map of the indirect exciton PL intensity versus the in-plane coordinate x and energy at T=1.6 K(**a**) and T=15 K (**c**). The temperature dependence

of the diameter of the indirect exciton cloud and their PL peak intensity are shown in **b** and **d**. As the temperature is reduced the indirect excitons condense at the bottom of the trap.

### 2.3 Stimulated Scattering of Indirect Excitons in CQWs[10]

The basic property of BE quantum statistics is the stimulated scattering: The scattering rate of bosons to a state  $\mathbf{p}$  is proportional to  $(1+N_{\mathbf{p}})$ , where  $N_{\mathbf{p}}$  is the occupation number of the state  $\mathbf{p}$ . At high  $N_{\mathbf{p}} \gg 1$  the scattering process is stimulated by the presence of other identical bosons in the final state. The stimulated scattering is a signature of quantum degeneracy and yields unambiguous evidence for the bosonic nature of excitons. In fact, observation of stimulated scattering requires less restricted experimental conditions than those necessary for BEC: With reducing temperature

and/or increasing density of excitons, the occupation numbers of the low energy states increase and the scattering arises as a precursor of the BEC or BEC-like phase transition. The latter is expected for interacting quasi-two-dimensional (2D) excitons.

The PL kinetics of indirect excitons is shown in Fig. 4. At low optical excitations, after a rectangular excitation pulse is switched off, the PL intensity of indirect excitons decays nearly mono-exponentially. To be noticed, there is a huge jump right after the excitation pulse is switched off with high power excitation (Fig. 4(a)). The rate,  $\tau_{rise}^{-1}$ , of the PL intensity enhancement increases strongly with increasing exciton density or lowering temperature (Fig. 4(b)).

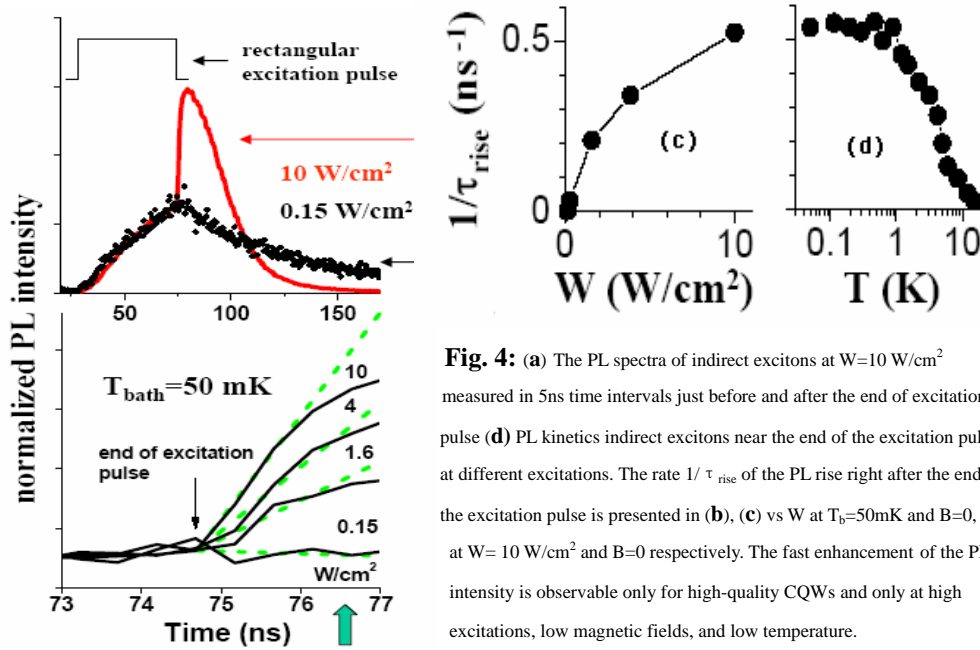


**Fig. 4:** (a) The PL spectra of indirect excitons at  $W=10 \text{ W/cm}^2$  measured in 5ns time intervals just before and after the end of excitation pulse (d) PL kinetics indirect excitons near the end of the excitation pulse at different excitations. The rate  $1/\tau_{rise}$  of the PL rise right after the end of the excitation pulse is presented in (b), (c) vs  $W$  at  $T_b=50\text{mK}$  and  $B=0$ ,  $T_b$  at  $W=10 \text{ W/cm}^2$  and  $B=0$  respectively. The fast enhancement of the PL intensity is observable only for high-quality CQWs and only at high excitations, low magnetic fields, and low temperature.

The time-integrated PL intensity remains almost constant with  $V_g$  variation, while the decay time changes by several orders of magnitude [12]. Hence, radiative recombination is the dominant mechanism of the decay of indirect excitons in the high-quality samples studied. For delocalized, in-plane free, 2D excitons only the states with small center-of-mass momenta  $|\mathbf{p}_{\parallel}| < p_0 \sim E_g \sqrt{\epsilon_b} / c$  ( $E_g$  is the band gap and  $\epsilon_b$  is the background dielectric constant) can decay radiatively by resonant emission of bulk photons [13] (see Fig. 5(b)). Thus the PL dynamics is determined by the occupation kinetics of the optically active low-energy states  $E < E_{p_0}$  ( $E_{p_0}/k_B = p_0^2/2M_x k_B \sim 1.2\text{K}$  at  $B=0$ ). The LA-phonon-assisted relaxation of hot photo-excited indirect excitons into the optically active low-energy states results in a rise of the PL signal, while optical recombination of the low-energy indirect excitons results in decay of PL intensity. The end of the excitation pulse is accompanied by a sharp drop of the

exciton temperature caused by the switching off the hot exciton generation and, as a result, the PL intensity and the occupation numbers  $N_E < E_{p0}$  abruptly rise within a few nanoseconds right after the trailing edge of the excitation pulse. The changes of the rate  $\tau_{rise}^{-1}$  of the PL intensity enhancement with varying exciton density, temperature (Figs.\*\*\*\*) correspond to changes of the LA-phonon-assisted exciton scattering rate to the optically active exciton states.

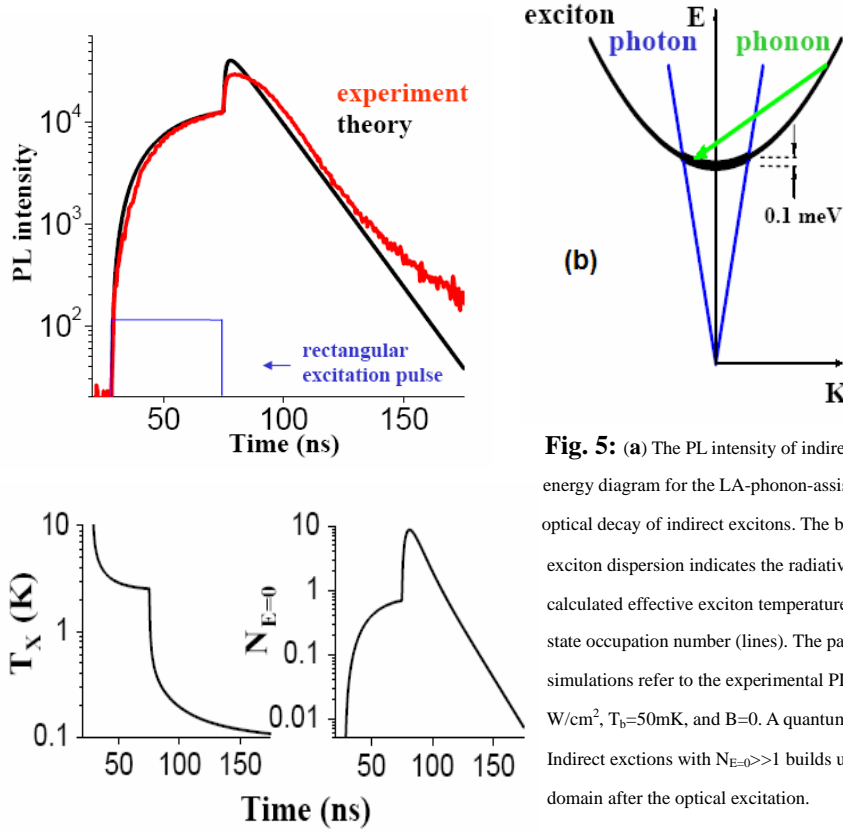


**Fig. 5:** (a) The PL intensity of indirect excitons, (b) energy diagram for the LA-phonon-assisted relaxation and optical decay of indirect excitons. The bold sector of the exciton dispersion indicates the radiative zone. (c) The calculated effective exciton temperature, and (d) the ground-state occupation number (lines). The parameters used in the simulations refer to the experimental PL kinetics at  $W=10$   $W/cm^2$ ,  $T_b=50$  mK, and  $B=0$ . A quantum degenerate gas of Indirect excitons with  $N_{E=0} \gg 1$  builds up in a few ns time domain after the optical excitation.

$$\begin{aligned}
 \frac{dN_{E=0}}{dt} &= \Gamma_{ph} N_E (1 + N_{E=0}) (1 + n_E^{ph}) - \Gamma_{ph} (1 + N_E) N_{E=0} n_E^{ph} - N_{E=0} / \tau \\
 &= \Gamma_{ph} (N_E - n_E^{ph}) N_{E=0} + \Gamma_{ph} (1 + n_E^{ph}) N_E - N_{E=0} / \tau
 \end{aligned} \quad (1)$$

As shown in the formula (1), the change rate of occupancy number in the low energy states is determined by three processes: increase due to the scattering from high energy state exciton via phonon emission, decrease due to the excitons scattered to high energy state via phonon absorption and from the radiative recombination. Right after the excitation pulse, more and more excitons are cooled down to the low energy state due to the sharp drop in the exciton temperature, which, in turn, is a positive feedback for the condensation. Thus there should be huge jump for the PL spectra at the pulse edge. In all, this behavior is just a signature of a degenerate Bose gas of indirect excitons.

## 2.4 Macroscopically ordered state [14]

The most remarkable consequence of BEC of a vast number of particles is that macroscopic properties become dependent on a single wave-function, promoting quantum physics to classical length and time scales. A BEC is a highly ordered state in which the wave-function phase is coherent over distances much longer than the separation between individual particles. Long-range quantum phase coherence has many dramatic physical consequences of which the most spectacular is superfluidity, ie, the ability to flow around obstacles with extremely weak, often immeasurable, dissipation. As for the excitons, theorists predicted such a phase transition to a coherent state due to the spontaneous symmetry breaking long time ago. However, there is little experimental achievement until recent years.

Here, the spatially and spectrally resolved PL experiments are intensively explored. It is amazing that a ring structure has been observed in the indirect exciton PL and a macroscopically ordered state appears in the ring that is farthest from the excitation spot (Fig. 6).

At lowest excitation powers,  $P_{\text{ex}}$ , the spatial profile of the indirect exciton PL intensity closely follows the laser excitation intensity. However, at high  $P_{\text{ex}}$  we observed a nontrivial pattern of that profile. The pattern is characterized by a ring structure (Fig. 6): the laser excitation spot is surrounded by two concentric bright rings separated by an annular dark intermediate region. The rest of the sample outside the external ring is dark. The internal ring appears near the edge of the laser excitation spot. Its radius increases with  $P_{\text{ex}}$ . The ring structure follows the laser excitation spot when it is moved over the whole sample area. This nontrivial spatial profile of the indirect exciton PL intensity is only observed at low temperatures. When the temperature is increased the bright rings wash out, the PL intensity in the inter-ring region and outside the external ring increases, and the profile approaches a monotonic bell-like shape.

The external ring is fragmented into circular structures that form a periodic array over macroscopic lengths, up to around 1mm (Fig. 6). This is demonstrated in Fig. 7(e) which shows the nearly linear dependence of the fragment positions along the ring versus their number. The fragments follow the external ring either when the excitation spot is moved over the sample area or when the ring radius varies with  $P_{\text{ex}}$ . Along the whole external ring, both in the peaks and the passes, the indirect exciton PL lines are spectrally narrow with the full-width at half-maximum (FWHM)  $\sim 1.3\text{meV}$ , considerably smaller than in the centre of the excitation spot; see Fig. 6(f). The ring fragmentation is observed at the lowest temperature only,  $T < 4\text{K}$  (Fig. 7(a)). With increasing temperature, the PL contrast along the ring washes out; this is quantified by the amplitude of the Fourier transform of the PL intensity variation along the ring (Fig. 7(d))

The spatial pattern shows also that the indirect exciton PL intensity is strongly enhanced in certain fixed spots on the sample; see Fig. 6(a, b, c, d). We call them localized bright spots (LBS). For any excitation spot location and any  $P_{\text{ex}}$  the LBS are only observed within the area terminated by the external ring. In the LBS the

indirect exciton PL line is spectrally narrow, the FWHM~1.2meV, and its energy is locally reduced. The LBS also wash out with increasing temperature.

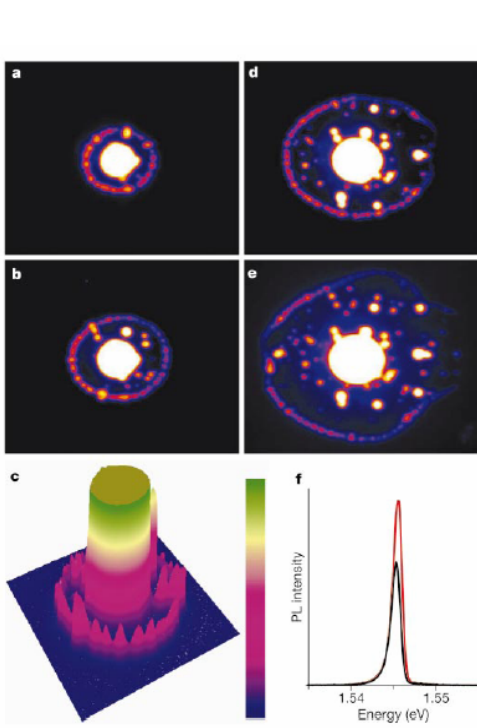


**Fig. 6:** Excitation density dependence of the spatial pattern of the indirect exciton PL intensity. **a-e**, The pattern at  $T=1.8\text{K}$ ,  $V_g=1.22\text{V}$  and  $P_{ex}=290$  (**a**),  $390$  (**b, c**),  $690$  (**d**), and  $1030$  (**e**)  $\mu\text{W}$ . For **a, b, d** and **e** the area of view is  $530 \times 440 \mu\text{m}$ . The external ring of the indirect exciton PL is fragmented into a periodic chain of circular structures. The fragments follow the external ring both when its radius is changed by varying  $P_{ex}$  or when the laser excitation is moved over the sample area. The indirect exciton PL intensity is also strongly enhanced in some spots within the area terminated by the external ring. The position of these spots is fixed on the sample. **f**, Indirect exciton PL spectra in a peak (red) and the adjacent pass (black) on the fragment chain along the ring. Color bar in **c** starts from zero (blue), and presents a linear scale.

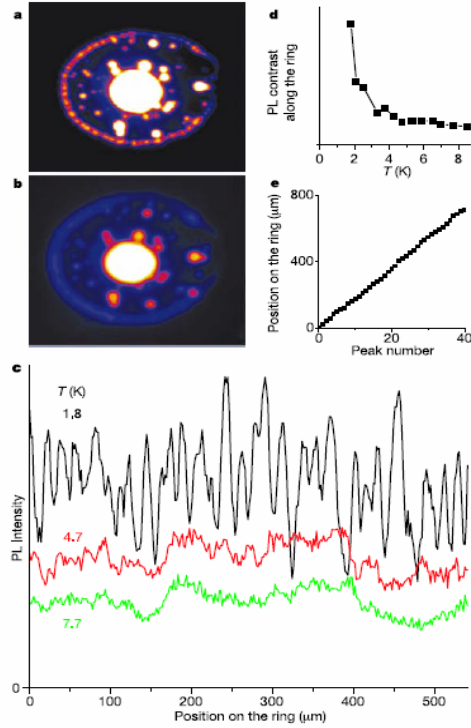


**Fig. 7:** Temperature dependence of the spatial pattern of the indirect exciton PL intensity. **a, b**, The pattern at  $T=1.8$  (**a**) and  $4.7\text{K}$  (**b**) for  $V_g=1.22\text{V}$ , and  $P_{ex}=690\mu\text{W}$ . The area of view is  $475 \times 414 \mu\text{m}$ . **c**, The corresponding variation of the indirect Exciton PL intensity along the external ring at  $T=1.8, 4.7$ , and  $7.7\text{K}$ . The ring fragmentation into the periodic chain washes out with increasing temperature. This is visualized by the PL contrast (**d**) presented by an amplitude of the Fourier transform. The dependence of the position of the indirect exciton PL intensity peaks along the external ring versus the peak number is nearly linear (**e**), showing that the fragments form a periodic chain.

To explain the dark region between the rings, it is proposed that excitons acquire an average drift momentum,  $K_{drift}$  when traveling out of the potential energy hill at the centre of the excitation spot. As the height of the potential energy hill at several milli-electron-volts is much larger than the kinetic energy at the radiative zone edge ( $\hbar^2 K_0^2 / (2M) \approx 0.1\text{meV}$ ),  $K_{drift}$  can exceed  $K_0$ . That means the moving excitons become optically inactive. This explains the existence of the dark region between the internal and external rings. Far from the excitation spot the main driving force for excitons relax down to the lowest energy states. This results in the sharp

enhancement of the radiative zone occupation and thus the PL intensity, and that is seen as the external ring. If this is true, it should be accompanied by that the optically inactive excitons move at speed faster than the speed of sound,  $v_s=3.7*10^5$ cm/s: even at  $K=K_0$ , the speed of the excitons is  $v = \hbar K_0 / M = 1.4 \times 10^6$  cm / s

However, there are different opinions on the origin of the dark region and the external ring. It is suggested that off-resonance laser excitation creates charge imbalance in CQWs, where electrons and holes have different collection efficiency. The holes deplete electrons in the vicinity of the laser spot, which creates hole rich and electron free region. Excitons are just generated with the interface between the hole rich region and the outer electron rich area, which arises the external ring.

The most interesting feature of the external ring is its fragmentation into a periodic array. The existence of periodic ordering shows the exciton state formed in the external ring has coherence on a macroscopic length scale. The coherence is not driven by a laser excitation because in the experiment the photo-excited carriers experience many inelastic scatterings before the optically active indirect excitons are formed. Instead, the coherence spontaneously appears in the exciton system. Especially, the macroscopic ordering is observed in the same temperature region as bosonic stimulated scattering, below a few kelven.

Comparing with the known phenomena, one may suggest that the fragments are vortices in the exciton system and that the ordering is the consequence of a repulsive interaction between the vortices. Within this model, the vortex rotation is continuously supported by the exciton flow out of the excitation spot. Similar to the arrays of vortices in the atom BECs, the rotation can be initiated even without an apparent external torque (possibly by a small variation from axial symmetry of the exciton flow due the in-plane potential fluctuations, which could cause a branching of the exciton flow, perhaps similar to the branching observed for the electron flow).

### III. Summary & Discussion

In part II, three experiments are stated to explore Bose Einstein condensation in the quasi-2D coupled quantum wells and its property. Actually, in infinite ideal 2D system BEC is only possible at  $T=0$ . However, in such a system, a related phase transition known as the Kosterlitz-Thouless superfluid (KTS) transition can occur [16]. In this case, spontaneous phase coherence of the particles occurs but does not persist to infinite range. The physical basis for BEC and KTS phase transition is the same: The bosonic particles prefer to be in the same quantum states, which leads to spontaneous phase correlation. The PL and its kinetic measurement just indicates the condensation to be a generate Bose gas of excitons in CQWs.

As for the macroscopic ring structure, we should note that a spontaneous macroscopic flow organization with periodic vortical structures is a general property of the thermodynamically open systems, both quantum and classical, described by nonlinear partial differential equations. A soliton array is another know phenomenon

that may be related to the macroscopically ordered exciton state. Multiple solitons are known to be stationary solutions of the nonlinear Schrodinger equation on a ring [17]. As the fragmentation appears abruptly at low temperatures, its nature is probably non-classical. Meanwhile, the microscopic nature of this ordered exciton state is not clear and warrents future studies. Furthermore, careful investigation on quantum hall effect of the excitons in CQWs may be beneficial for a deeper understanding of excitons behaviors at low temperature.

#### **IV. Reference**

1. Yarmchuk, E.J., Gordon, M. J.V. & Packard, R.E., Phys. Rev. Lett. 43, 214 (1979).
2. E.A. Cornell, C.E. Wieman, Rev. Mod. Phys. 74, 875(2002).
3. Madison, K.W., Chevy, F., Wohlleben, W. & Dalibard, J., Phys. Rev. Lett. 84, 806 (2000).
4. Essmann, U. & Trauble, H., Phys. Lett. A 24, 526(1967).
5. Keldysh, L.V. & Kozlov, A.N., Sov. Phys. JETP 27, 521(1968).
6. Perakis, I.D., Naure 417, 33(2002).
7. Snoke, D.W., Wolfe, J.P. & Mysyrowicz, A., Phys. Rev. Lett. 59, 827(1987).
8. Lin, J.L. & Wolfe, J. P., Phys. Rev. Lett. 71, 1222(1993).
9. O' Hara, K.E., Suilleabhain, L.O. & Wolfe, J.P., Phys. Rev. B 60, 10565(1999).
10. L.V. Butov, A.L. Ivanov & A. Imamoglu, Phys. Riew. Lett. 86, 5608(2001).
11. L.V. Butov, C.W. Lai & A.L. Ivanov, Nature, 417, 47(2002).
12. L.V Butov, A. Imamoglu, S.V. Mintsev, K.L Campman & A.C. Gossard, Phys. Rev. B 59, 1625(1999).
13. J. Feldmann, G. Peter, E.O. Göbel, P. Dawson, K. Moore, C. Foxon, and R.J. Elliott, Phys. Rev. Lett. 59, 2337(1987).
14. L.V. butov, A.C. Gossard & D.S. Chemla, Nature 418, 751(2002).
15. David Snoke, Scinece 298, 1368 (2002).
16. J.M. Kosterlitz, D.J. Thouless, J. Phys. C Solid state Phys. 6, 1181(1973).
17. Carr, L.D., Clark, C.W. & Reinhardt W.P., Phys. Rev. A 62, 063610-1(2000).